Brandolin, G., Dupont, Y., & Vignais, P. V. (1981) *Biochem. Biophys. Res. Commun. 98*, 28–35.
Brandolin, G., Dupont, Y., & Vignais, P. V. (1982) *Biochemistry 21*, 6348–6353.
Butler, P. J. G., & Hartley, B. S. (1972) *Methods Enzymol. 25*, 191–199.
Cabral, F., & Schatz, G. (1979) *Methods Enzymol. 56*, 602–613.
Chang, J. Y. (1979) *Biochim. Biophys. Acta 578*, 188–195.
Chin-Sun, W., & Smith, R. L. (1975) *Anal. Biochem. 63*, 414–417.
Dalbon, P., Boulay, F., & Vignais, P. V. (1985) *FEBS Lett. 180*, 212–218.
Dulley, J. R., & Grieve, P. A. (1975) *Anal. Biochem. 64*, 136–141.
Gilles, A.-M., Imhoff, J.-M., & Keil, B. (1979) *J. Biol. Chem. 254*, 1462–1468.
Gross, E. (1967) *Methods Enzymol. 11*, 238–255.
Hoppe, J., & Sebald, W. (1980) *Eur. J. Biochem. 107*, 57–65.
Hoppe, J., Gatti, D., Weber, H., & Sebald, D. W. (1986) *Eur. J. Biochem. 155*, 259–264.
Horn, M. J., & Laursen, R. A. (1973) *FEBS Lett. 36*, 285–288.
Klotz, I. M. (1967) *Methods Enzymol. 11*, 576–580.
Lauquin, G. J. M., & Vignais, P. V. (1976) *Biochemistry 15*, 2316–2322.
Lauquin, G. J. M., Villiers, C., Michejda, J. W., Hryniewiecka, L. V., & Vignais, P. V. (1977) *Biochim. Biophys. Acta 460*, 331–341.
Müller, W., & Amons, R. (1985) *FEBS Lett. 186*, 1–7.
Müller, M., Krebs, J. J. R., Cherry, R. J., & Kawato, S. (1984) *J. Biol. Chem. 259*, 3037–3043.
Patterson, M. S., & Greene, R. C. (1965) *Anal. Biochem. 37*, 854–857.
Riccio, P., Aquila, H., & Klingenberg, M. (1975) *FEBS Lett. 56*, 133–138.
Runswick, M. J., Powell, S. J., Nyren, P., & Walker, J. E. (1987) *EMBO J. 6*, 1367–1373.
Saraste, M., & Walker, J. E. (1982) *FEBS Lett. 144*, 250–254.
Schenkein, I., Levy, M., Franklin, E. C., & Frangione, B. (1977) *Arch. Biochem. Biophys. 182*, 64–70.
Smith, A. L. (1967) *Methods Enzymol. 10*, 81–86.
Torok, K., & Joshi, S. (1985) *FEBS Lett. 182*, 340–344.
Vignais, P. V., Block, M. R., Boulay, F., Brandolin, G., & Lauquin, G. J. M. (1985) in *Structure and Properties of Cell Membranes* (Bengha, G., Ed.) Vol. II, pp 139–179, CRC, Boca Raton, FL.
Walker, J. E., Saraste, M., Runswick, M. J., & Gay, N. J. (1982) *EMBO J. 1*, 945–951.
Weidemann, M. J., Erdelt, H., & Klingenberg, M. (1970) *Eur. J. Biochem. 16*, 313–335.
Zak, B., & Cohen, J. (1961) *Clin. Chim. Acta 6*, 665–670.

Structure Elucidation of the Blood Group B Like and Blood Group I Active Octaantennary Ceramide Tetracontasaccharide from Rabbit Erythrocyte Membranes by Two-Dimensional ^{1}H NMR Spectroscopy at 600 MHz†

Janusz Dabrowski* and Ursula Dabrowski
Max-Planck-Institut für Medizinische Forschung, D-6900 Heidelberg, West Germany
Wolfgang Bermel
Bruker Analytische Messtechnik, D-7512 Rheinstetten 4, West Germany
Maria Kordowicz and Peter Hanfland
Institut für Experimentelle Hämatologie und Bluttransfusionswesen, Universität Bonn, D-5300 Bonn 1, West Germany
Received September 22, 1987; Revised Manuscript Received February 25, 1988

ABSTRACT: The primary structure of the ceramide tetracontasaccharide (**1**) from rabbit erythrocyte membranes has been determined with the aid of 600-MHz two-dimensional phase-sensitive correlated, "totally correlated" (TOCSY, homonuclear Hartmann–Hahn), relayed coherence transfer, triple quantum filtered, and nuclear Overhauser enhancement ^{1}H NMR spectra. It was shown that obtaining subspectra of the constituent sugar residues from a totally correlated spectrum and assigning the resonances occurring in these subspectra by analyzing the relevant cross-peaks in phase-sensitive correlated spectra is the most efficient way for establishing complex oligosaccharide structures. This analysis has shown **1** to be the highest homologue of the multiantennary neolactoglycosphingolipids of the following general formula with $n = 7$:

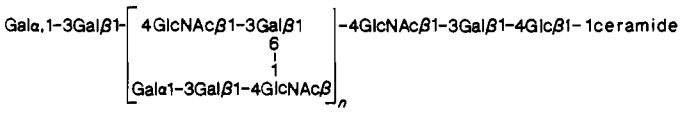

In previous papers from our laboratories the isolation, structure determination, and properties of the biantennary (Hanfland et al., 1981), triantennary (Dabrowski et al., 1984), and tetra- and pentaantennary (Hanfland et al., 1988) neolactoglycosphingolipids of the general formula given under Abstract have been described. It was pointed out that blood group I activity of these compounds increases along with increasing branching of their oligosaccharide skeleton. Recently, we reported on the isolation of hexa-, hepta-, and octaan-

† Supported by the Fritz Thyssen Stiftung (J.D. and U.D.), the Fonds der Chemischen Industrie (J.D.), and the Deutsche Forschungsgemeinschaft, Grant Ha 627/2-2 (M.K. and P.H.). This is part of the series "Immunochemistry of I/i Active Oligo- and Polyglycosylceramides from Rabbit Erythrocyte Membranes".

0006-2960/88/0427-5149$01.50/0

tennary species from the same source, i.e., from rabbit erythrocyte membranes (Kordowicz et al., 1986). The title octaantennary glycosphingolipid (**1**) composed of 40 sugar residues appears to be the largest oligosaccharide of defined size obtained to date. The purpose of this work is to show that its structure can be determined with the aid of the newer methods of two-dimensional (2D) ^{1}H NMR[1] spectroscopy applied at 600 MHz, which is the highest frequency accessible at present. In view of the complexity of this task and because of the relative novelty of the techniques used, it is believed that the assignment strategies employed can be of general utility in work on structure elucidation of complex carbohydrates.

Structural information obtainable by various modern one- and two-dimensional multipulse NMR techniques is often redundant; hence, when approaching the determination of a complex structure, one should carefully select the appropriate assignment strategy in order to save instrumental and processing time. With any strategy, one has first to perform a connectivity analysis in order to determine the number of different spin systems, corresponding to sugar residues that either are different themselves or are the same but located in different environments. The presence of identical sugar units situated in indistinguishable environments can be shown by integration of the 1D spectrum. The next task is to identify all these residues, and to this end, the vicinal coupling constants around each of the sugar rings are required. It is desirable, therefore, to obtain information on chemical shift connectivities and coupling patterns possibly in one experiment. Although a number of methods are potentially useful for this purpose, it is difficult to predict which will be the optimum one in a given case, since the NMR observables are functions of many variables depending on both the parameters used in the experiment and the properties of the molecules investigated. In our experience, pure absorption phase-sensitive correlation spectroscopy (PS-COSY; Marion & Wüthrich; 1983; Rance et al., 1983) is the method of choice for native (Romanowska et al., 1987; Dabrowski et al., 1988) and peracetylated (Dabrowski et al., 1987) oligosaccharides of medium size. However, with more complex oligosaccharides, particularly the native ones, the connectivities become equivocal, owing to too many degeneracies of chemical shifts in the signal envelope comprising virtually all nonanomeric proton resonances. We suggest here a two-step procedure to resolve this problem. First, subspectra of all of the constituent sugar residues are extracted from a 2D homonuclear Hartmann–Hahn (HOHAHA) spectrum (Müller & Ernst, 1980; Davis & Bax, 1985). Second, each of the sugar resonances in a given subspectrum is identified by analyzing the fine structure of the relevant PS-COSY cross-peaks. It may be desirable or even necessary to complement or confirm the results thus obtained, and for this purpose the triple quantum filtered (TQF) COSY (Piantini et al., 1982) and relayed coherence transfer (RCT; Eich et al., 1982) spectra can be applied. The former enables one to virtually remove all but those signals that belong to three mutually coupled protons (i.e., sugar H5, H6, and H6′ and ceramide H1, H1′, and H2 in the case of **1**). The usefulness of such simplified spectra for structural analysis of carbohydrates has recently been demonstrated (Hikichi, 1984; Homans et al., 1986; Dabrowski, 1987; Dabrowski et al., 1987, 1988).

[1] Abbreviations: DQF, double quantum filtered; 1D and 2D, one and two dimensional; Gal, galactose; Glc, glucose; GlcNAc, 2-acetamido-2-deoxyglucose; HOHAHA, homonuclear Hartmann–Hahn spectroscopy; NMR, nuclear magnetic resonance; NOESY, two-dimensional nuclear Overhauser effect spectroscopy; PS, phase sensitive; TOCSY, total correlation spectroscopy; TQF, triple quantum filtered.

The elucidation of the primary structure is completed by the determination of the sites of glycosidic linkages and of the sequence, which can be achieved with the aid of the nuclear Overhauser effect [Hanfland et al., 1981; Prestegard et al., 1982; for other references, see Dabrowski (1987) and Koerner et al. (1987)].

Experimental Procedures

The preparation of **1** was described previously [Kordowicz et al. (1986) and references cited therein]. For ^{1}H NMR measurements, 10 mg of deuterium-exchanged **1** was dissolved in 0.35 mL of Me_2SO-d_6 containing 2% D_2O. Spectra were obtained at a frequency of 600 MHz and a temperature of 333 K on a Bruker AM-600 spectrometer equipped with an Aspect 3000 computer and an array processor. Chemical shifts were referenced indirectly to Me_4Si by setting the ^{1}H signal of Me_2SO-d_5 at 2.49 ppm.

The one-dimensional (1D) spectrum was recorded with a repetition interval of 10 s applied for optimum integration. The NOE difference spectrum was obtained as described by Wagner and Wuthrich (1979).

The relaxation delay for all 2D-spectra was 2s, and the spectral width was 2060 Hz.

The HOHAHA spectrum was recorded according to the method described by Davis and Bax (1985), with a total spin-lock duration of 100 ms. The time-domain data matrix containing 1K × 512 points was multiplied by phase-shifted ($\pi/6$ in t_2 and $\pi/3$ in t_1) sine bell functions and zero-filled to 4K × 1K points. Accordingly, digital resolution in the frequency domain was 1.0 and 2.0 Hz per point in ω_2 and ω_1, respectively.

The PS-COSY spectrum with pure-absorption line shapes was obtained with the use of time-proportional phase increments (Marion & Wuthrich, 1983) and double quantum filtering (DQF; Piantini et al., 1982; Rance et al., 1983). The matrix size was 4K × 1K; 16 transients for each t_1 were accumulated. These data were multiplied by shifted sine bell window functions (phase shifts of $\pi/8$ in t_2 and $\pi/4$ in t_1) and zero-filled in both dimensions. After Fourier transformation the final digital resolutions were 0.50 and 1.0 Hz per point in the ω_2 and ω_1 dimensions, respectively.

The NOESY spectrum was obtained in phase-sensitive mode (Bodenhausen et al., 1984), with 32 transients per t_1 accumulated. No random variation of the mixing delay (0.3 s) was applied. The matrix size was 4K × 1K (4K × 2K after zero filling), and the final digital resolution was 1.0 Hz per point. Prior to Fourier transformation, a phase-shifted ($\pi/8$ in t_2 and $\pi/4$ in t_1) sine bell apodization was applied.

The size of the time-domain data matrices was 2048 × 512 for delayed COSY, RCT, RCT-2, RCT-3, and TQF-COSY spectra. The data were multiplied by sine bell weighting functions in both dimensions, zero filled in t_1, and Fourier transformed. The final digital resolution was 2.0 Hz per point.

For all RCT spectra (Eich et al., 1982), refocusing delays of 30 ms were given. For each t_1 value, 16 transients for RCT and RCT-2 and 32 transients of RCT-3 were collected. The TQF-COSY spectrum (Piantini et al., 1982) was obtained by accumulating 16 transients for each t_1.

Results and Discussion

The 1D 600-MHz ^{1}H NMR spectrum of **1** (Figure 1) differs little from the 500-MHz spectra of the lower homologues of the multiantennary neolactoglycosphingolipids (Hanfland et al., 1981, 1988; Dabrowski & Hanfland, 1982; Dabrowski et al., 1984), except for the integrals of several peaks to be discussed later. The HOHAHA and the PS-C-

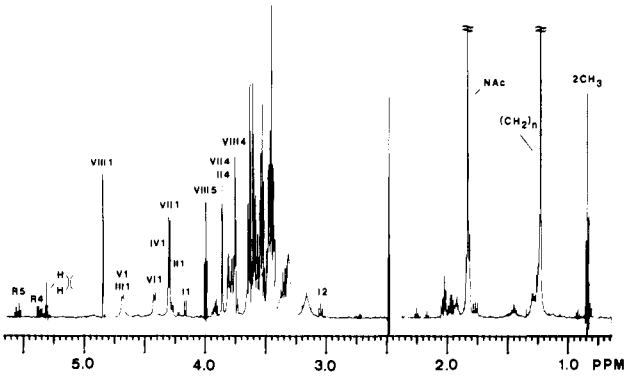

FIGURE 1: Resolution-enhanced 600-MHz ^{1}H NMR spectrum of ceramide tetracontasaccharide (**1**) in Me_2SO-d_6/D_2O (49:1) at 333 K. For labeling, cf. the formula in Table I, but ceramide residue = R.

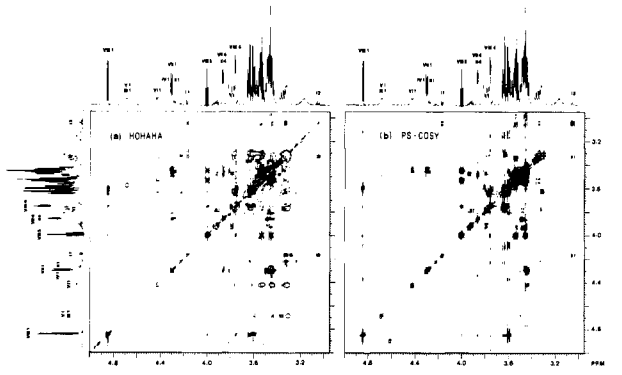

FIGURE 2: Sugar proton region of the 600-MHz HOHAHA (a) and PS-COSY (b) spectra of **1** (cf. legend of Figure 1).

OSY spectrum are shown in Figure 2.

To condense the evaluation of the experimental data, the labeling of the sugar residues, which will follow from the entire assignment procedure, is being used here in advance.

It may seem that the most reliable way to assign proton resonances in the subspectra of the component sugar residues is to consecutively record COSY and RCT-1, -2, etc. spectra, or their 1D variants (Perly et al., 1987), whereby H2, H3, H4, etc. chemical shifts would be succesively defined. However, the RCT pulse sequence, $90–t_1–[90–\tau_i–180–\tau_i]_n–90–$acquire, includes two delays (τ_i) for each n step, with τ_i being inversely proportional to the coupling constant between the protons exchanging coherence during the given step; thus, the net signal obtained in a multistep experiment may be weak, or even disappear, particularly if (a) one or more of the coupling constants are small and (b) the effective transverse relaxation time (T_2^*) is short. The decisive role of T_2^* is clearly illustrated by the RCT subspectra of the Gal-VIII and GlcNAc-VI residues. Whereas all of the seven protons of Gal-VIII can unequivocally be assigned by combining the RCT-3 cross sections through its H1 and H5 resonances (3a, b), the RCT signals for GlcNAc-VI are weak in the RCT-2 spectrum (Figure 4b) and altogether absent from the RCT-3 one (not shown). No doubt, T_2^* for GlcNAc-VI is short, owing to some exchange process, as can be inferred from the broadening of the anomeric proton signal in the 1D spectrum (Figure 1). In contrast, magnetization transfer through the entire spin system of a sugar residue is sufficiently effective during the short spin-lock interval of the HOHAHA spectrum, as seen from the excellent signal-to-noise ratio in the HOHAHA subspectra of both Gal-VIII and GlcNAc-VI (Figures 3c,d and 4c, respectively). On the other hand, the fact that all of the signals were obtained in one step raises the question of their assign-

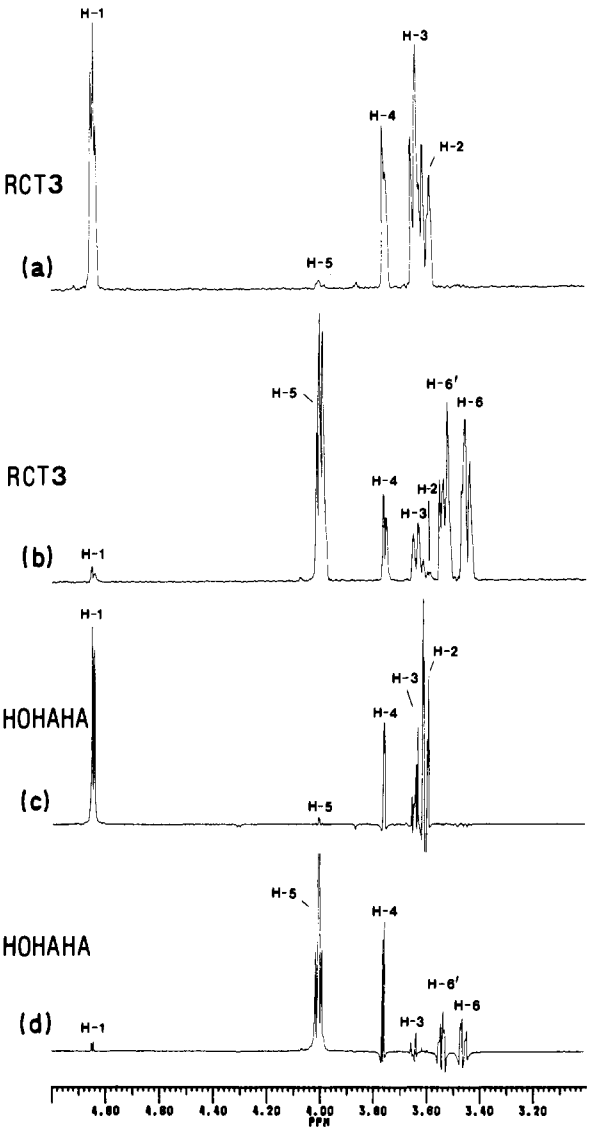

FIGURE 3: Subspectra of the Gal-VIII residues extracted from the 600-MHz RCT-3 (a and b) and HOHAHA (c and d) spectra of **1**. Cross sections through the H1 (a and c) and through the H5 (b and d) resonances.

ment. As pointed out in the introduction we suggest application of PS-COSY spectra for this purpose, and panels d–g of Figure 4 illustrate the approach.

The analysis of phase-sensitive COSY cross-peaks in sugar spectra has been described in some detail (Dabrowski, 1987; Dabrowski et al., 1987, 1988; Berman, 1987). In short, the fine-structure splitting that corresponds to the coupling between a pair of protons giving rise to the cross-peak in question (the so-called active coupling) appears in antiphase along both frequency axes (ω_1 and ω_2), whereas any coupling to side protons (passive coupling) appears as an additional in-phase splitting along the appropriate frequency axis. For example, the VI_3^4 cross-peak, which is situated at ω_2(H4) and ω_1(H3) shows, along ω_2, antiphase components spaced by $J_{3,4}$ and in-phase components separated by $J_{4,5}$ (Figure 4g); a cross section parallel to ω_1 (not shown) contains the same antiphase $J_{3,4}$ components, but the in-phase components are separated by $J_{2,3}$.

Of the seven multiplets seen in the HOHAHA subspectrum of the 1–6-linked GlcNAc-VI residue (Figure 4c), those for H1 and H2 can be directly assigned by their connectivity evidenced by the PS-COSY spectrum, the VI_1^2 cross-peak at ω_2(H2),ω_1(H1) defining simultaneously the $J_{2,3}$ coupling

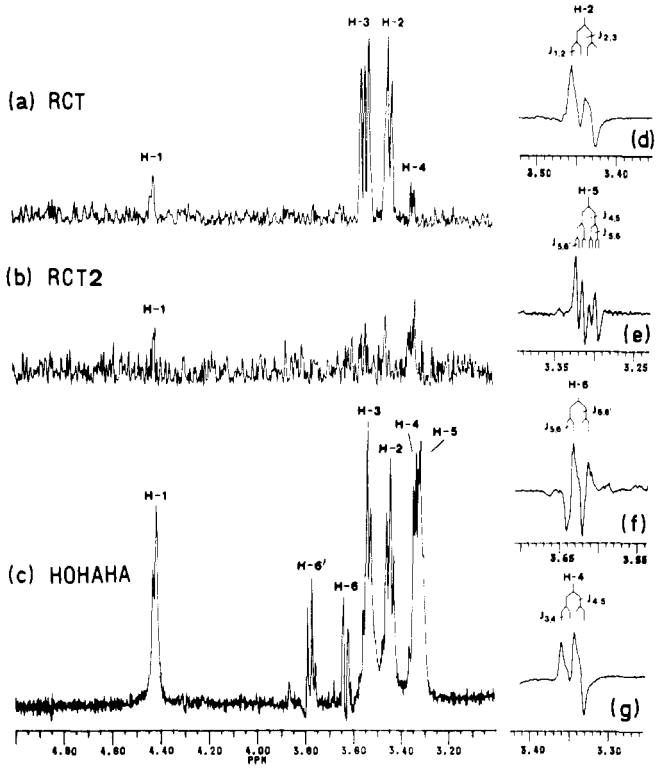

FIGURE 4: Cross-sections through the GlcNAc-VI H1 resonance of the RCT (a), RCT-2 (b), and HOHAHA (c) spectra and through the H2 (d), H5 (e), H6 (f), and H4 (g) resonances of the PS-COSY spectrum of **1**. A detailed interpretation is given in the text.

constant, which is passive in the cross-section drawn parallel to ω_2 (Figure 4d). H5 is the only proton coupled to three others; hence, it can readily be recognized by the 2^3 multiplet components in any of the cross sections, parallel to ω_2, through the VI_4^5, VI_6^5, or $VI_{6'}^5$ cross-peaks, which all occur at the H5 chemical shift in the ω_2 dimension. In fact, VI_4^5 was unsuitable because of the almost coincident H4 and H5 resonances, but the cross-section at ω_1(H6′) through the $VI_{6'}^5$ cross-peak is easily analyzable (Figure 4e). The antiphase splitting corresponds to $J_{5,6'}$ (active coupling), and the in-phase splitting reflects $J_{4,5}$ and $J_{5,6}$ (passive couplings). These two passive couplings can be distinguished by analyzing the cross section drawn at ω_1(H5), where $J_{5,6}$ is active in the VI_5^6 cross-peak at ω_2(H6) (Figure 4f), and the cross section traced at ω_1(H3) through the VI_3^4 cross-peak just discussed (Figure 4g), where $J_{4,5}$ is passive. The identity of $J_{4,5}$ determined from the $VI_{6'}^5$ and VI_3^4 cross-peaks provides the assignment of H4 and, indirectly, H3, and thus completes the analysis for this spin system. The assignment H3 can be confirmed by the multiplet structure of this proton resonance. Although this can, in principle, be done by analyzing the cross section, parallel to ω_1, through the same VI_3^4 cross-peak, one should rather take advantage of the better digital resolution along ω_2 and analyze the two VI_4^3 cross-peak (not shown).

When assigning the 1–3-linked GlcNAc residues, one should take into account their possible differentiation. Although all of them are 1–4 glycosylated by β-Gal residues and 1–3 linked to aglyconic β-Gal residues, there are small differences in their

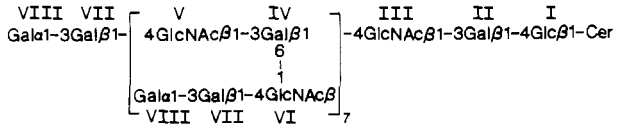

environments, which may result in different shielding. The distinguishing feature of GlcNAc-III is its unbranched aglycon; among the remaining 1–3-linked GlcNAc residues (labeled GlcNAc-V in the formula), one can formally distinguish between that glycosylated by the Galα1–3Galβ disaccharide unit of the sole 1–3-linked terminal branch and the six that are glycosylated by bifurcated residues. Thus, three sets of resonances can formally be expected for these three subtypes of GlcNAcβ1–3 residues. As will be shown below, however, only two such sets were found, one of them being attributable to GlcNAc-III and the other one to all of the GlcNAc-V residues. Although the broadened 1D H1 signal at 4.68 ppm appears symmetric (Figure 1), its minor high-field component is visible in the same spectrum processed with extreme resolution enhancement. This differentiation is unequivocally confirmed by the distinctly separated III_1^2 and V_1^2 PS-COSY cross-peaks (Figures 2a and 5a). The V_3^2 cross-peak is partly overlapped by t_1 noise, and the III_3^2 one is even more so; hence, the connectivities with the two H3 resonances need to be confirmed. Unfortunately, the minute difference of 0.005 ppm (3 Hz) in H1 chemical shifts results in overlapped HOHAHA subspectra of the GlcNAc-III and -V spin systems ("cross-talk" between the neighboring rows of the 2D matrix), showing undifferentiated H3 resonances at ~3.58 ppm (Figure 5b). This assignment is confirmed by the RCT spectrum, which shows an unresolved H1/H3 cross-peak, at ~4.68/3.58 ppm, pertaining to these two spin systems (Figure 5c). To trace the H3/H4 connectivities, one has first to return to the PS-COSY spectrum, where the two H3 chemical shifts are resolved, as follows from the occurrence of two H4/H3 cross-peaks at 3.361/3.588 and 3.380/3.576 ppm, respectively. It remains to establish the remote connectivities between the two H4 resonances thus found (3.361 and 3.380 ppm) and the H2 resonances assigned above. This question can be solved with the aid of HOHAHA cross sections (columns): that taken at 3.361 ppm (Figure 5d) clearly contains the V-2 signal at 3.433 ppm, along with a weak III-2 signal at 3.478 ppm (occurring because of cross-talk), whereas in the column taken at 3.380 ppm the V-2 signal is completely lacking and the III-2 signal is strong (Figure 5e). Furthermore, the H1 signals occur in these cross sections at 4.684 and 4.679 ppm, respectively, as expected for the assignments presented in Table I. The H5, H6, and H6′ resonances were readily assigned in the PS-COSY and HOHAHA spectra and confirmed by the TQF-COSY spectrum (Figure 6). The attribution of the minor component of 1–3-linked glucosamines to GlcNAc-III, as mentioned at the beginning of this paragraph, can be substantiated by interresidue NOEs between H1 of Gal-IV or -VII residues and the respective H4 protons just assigned. Thus, both in the 1D NOE difference spectrum obtained upon irradiation at 4.30 ppm and in the cross sections through this resonance in the 2D NOESY matrix, strong NOE signals are at ~3.35 ppm (H4 of the seven GlcNAc-VI and ~3.36 ppm (H4 of the seven GlcNAc-V), whereas only a shoulder occurs at ~3.38 ppm, as expected for H4 of the single GlcNAc-III.

Another problem of some complexity is the assignments of β-Gal residues IV and VII, whose H1 resonances are so close as not to be confidently distinguishable in the 1D spectrum, although, with extreme resolution enhancement, a broad doublet tends to separate on the low-field side of the ~4.30 ppm signal. In the HOHAHA spectrum, however, there are two widely separated H1/H4 cross-peaks, at 4.302/3.814 and 4.297/3.864 ppm (Figure 2a), each of which correlates with a different set of H5, H6, and H6′ protons, as indicated in Table I. Taking into account that glycosylation-induced shifts for protons at the glycosylation site and vicinal to it are toward lower field (Dabrowski et al., 1982), the set comprising low-

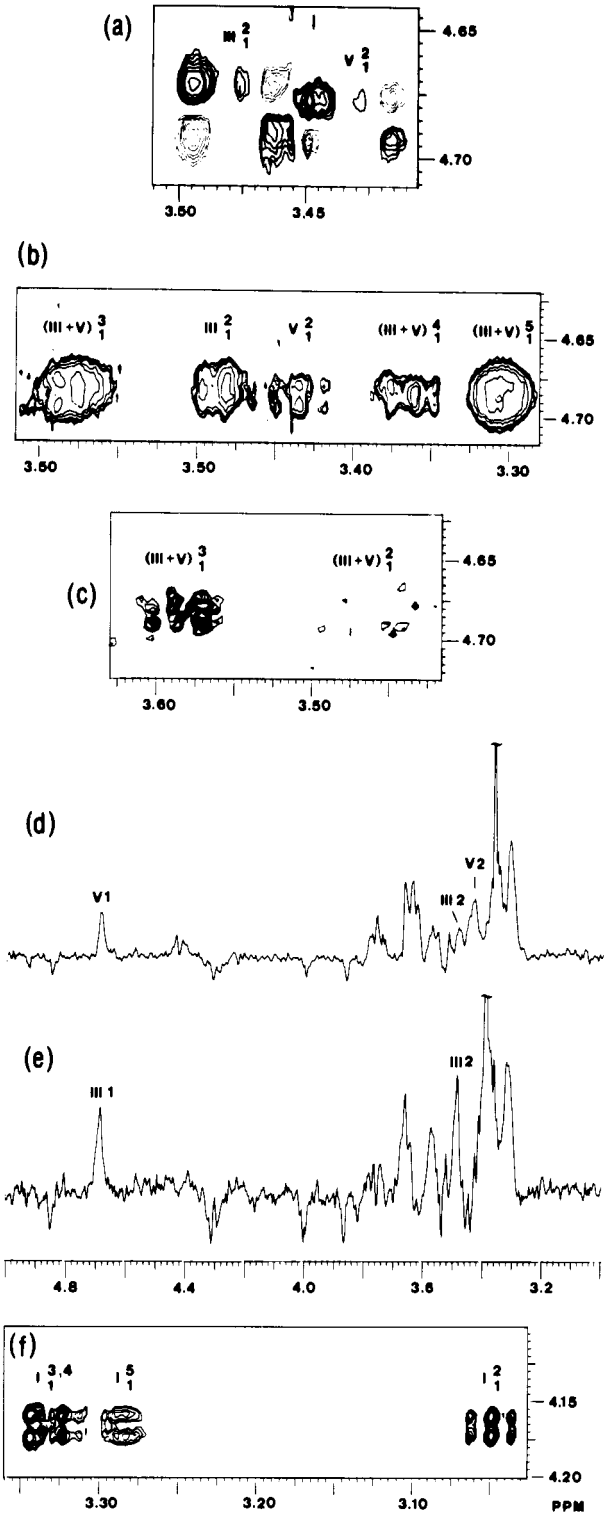

FIGURE 5: Spectral fragments referring to GlcNAc-III and -V (a–e) and Glc-I (f). (a) PS-COSY cross-peaks showing the H2/H1 connectivities. A Roman numeral denotes a sugar residue (as in Figure 1), its superscript denotes the proton whose chemical shifts is to be read on the ω_2 (horizontal) scale), and the subscript refers to the proton whose chemical shift defines the ω_1 coordinate (vertical scale). Positive and negative multiplet components are drawn in fat and thin lines, respectively. Note the cancellation of the middle antiphase components of each of the cross-peaks. (b) HOHAHA cross-peaks showing the connectivities of several protons, indicated by labels, with H1. Bracketed residue labels refer to undifferentiated cross-peaks. (c) RCT cross-peak for the undifferentiated H3/H1 connectivity. The H2/H1 cross-peak is nearly missing. (d) HOHAHA cross-section (column) at ω_2 = 3.361 ppm. (e) As in (d) but ω_2 = 3.380 ppm. (f) HOHAHA cross-peaks showing the connectivities of several Glc-I protons with its H1.

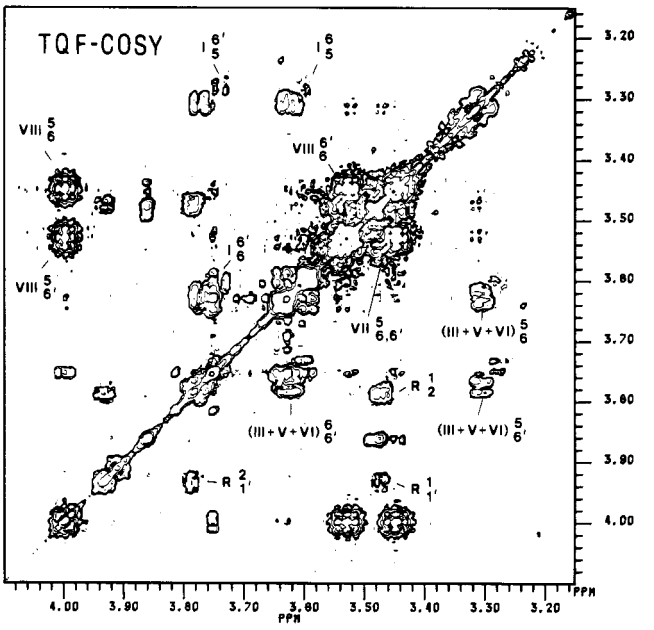

FIGURE 6: Nonanomeric proton region of the 600-MHz TQF-COSY spectrum of **1**. Labeling is as in Figure 5, and R = ceramide. To avoid crowding, only one cross-peak from each pair is labeled, either above (those for residues I and VIII) or below the diagonal (those for III, V, VI, and VII and R = ceramide).

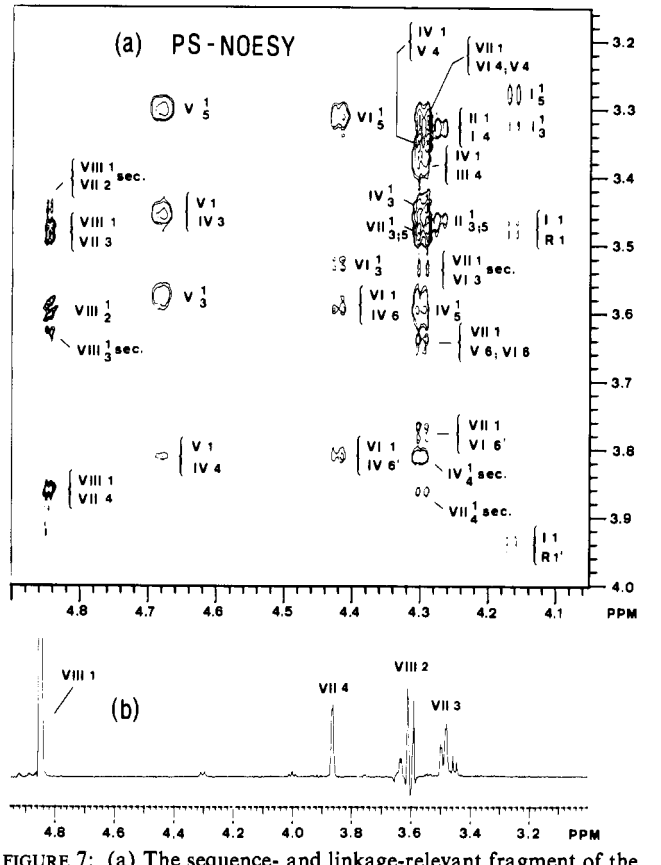

FIGURE 7: (a) The sequence- and linkage-relevant fragment of the 600-MHz NOESY spectrum of **1**. For the cross-peaks originating from *intra*residue NOE, e.g., VI^1_5, labeling is the same as in Figure 5, and R = ceramide. *Inter*residue NOEs are highlighted by braces. sec. means secondary NOE brought about by spin diffusion or by higher order coupling mechanisms. Cross-peaks referring to the I1 → 1R and I1 → 1′R through-space connectivities were weak and had to be reproduced from a lower level of the 2D matrix. (b) Cross-section through the H1 resonance of the Gal-VII residue.

field-shifted resonances obviously represents the 6-glycosylated Gal-IV residues. Since, owing to a small $^3J_{4,5}$ coupling constant and short transverse relaxation time T_2^* (Dabrowski, 1987),

Table I: Chemical Shifts (ppm from Me_4Si) and Coupling Constants (Hz) Measured at 600 MHz for a 4 mM Solution of Ceramide Tetracontasaccharide (**1**) in Me_2SO-d_6/D_2O (49:1) at 333 K

protons	Galα1-3Galβ1 4GlcNAcβ1			4GlcNAcβ1-3 6 Galβ1-4GlcNAcβ1-3Galβ1-4Glcβ1-1Ceramide[a]					
	VIII	VII	VI	V	IV	III	II	I	R[a]
H-1	4.843	4.297	4.421	4.684	4.302	4.679	4.274	4.167	3.475; 3.933[b]
H-2	3.598	3.442	3.442	3.433	3.44	3.478	3.454	3.051	3.787
H-3	3.638	3.487	3.538	3.588	3.46	3.576	3.462	3.337	3.912
H-4	3.753	3.864	3.348	3.361	3.814	3.380	3.860	3.33	5.376
H-5	3.998	3.474	3.310	3.300	3.605	3.300	3.474	3.281	5.553
H-6	3.452	3.543	3.627	3.627	3.582	3.627	3.543	3.606	1.931
H-6'	3.534	3.543	3.778	3.778	3.804	3.778	3.543	3.743	
$^3J_{1,2}$	3.8	7.9	8.3	9.4	7.9	10.3	7.9	7.8	3.7; 5.2[c]; 10.3[d]
$^3J_{2,3}$	10.2	9.5	11.2	10.8	8.1	9.6		8.9	8.9
$^3J_{3,4}$	3.6	3.4	7.5	7.7	4.3	9.9	3.4		6.4
$^3J_{4,5}$	1.8		10.1	10.0		10.0		9.2	
$^3J_{5,6}$	6.2		5.2	5.2		5.2		5.2	
$^3J_{5,6'}$	6.5		2.8	2.8		2.8			
$^2J_{6,6'}$	10.8		12.4	12.4		12.4		11.1	

[a] Numbering for the ceramide residue: $—CH_2^{1,1'}—CH^2[NHC(O)alkyl]—CH^3(OH)—CH^4{=}CH^5—CH_2^6—$alkyl. [b] Refers to H1'. [c] Refers to $^3J_{1',2}$. [d] Refers to $^2J_{1,1'}$.

the H4/H5 connectivity does not show up in any of the variants of scalar correlated spectra (COSY, delayed COSY, PS-COSY, RCT, or HOHAHA), it has to be shown how this critical relation between the H1–H4 and H5–H6′ spectrum fragments was established. First, the missing H4/H5 connectivity was observed in the NOESY spectrum thanks to the mutual gauche orientation of these two protons. Then, the correlations between the H5 resonance thus found and the H6 and H6′ ones were established in the PS-COSY spectrum. The assignments for Gal-VII were obtained in a similar way and confirmed by the interresidue NOEs VIII1/VII3 and VIII1/VII4 (vide infra) and by the TQF-COSY spectrum. Gal-II of the lactose head unit clearly differs from the other β-Gal units, V and VII, in H1 and H2 chemical shifts, wherefrom the further connectivities can be followed.

For Glc-I, the difficulty consisted in the almost degenerate H3 and H4 resonances. Nevertheless, the connectivities H1/H2/(H3 + H4)/H5 could readily be found in the HOHAHA spectrum (Figures 2a and 5f) and the analysis completed by finding the H5/H6/H6′ connectivities in the TQF-COSY spectrum (Figure 6).

α-Gal-VIII residues contrasted favorably with β-Gal ones in that the critical H4/H5 connectivity was directly visible in the PS-COSY spectrum (Figure 2b), owing to the fairly large H4/H5 coupling constant (1.8 Hz) and the higher mobility (hence, longer T_2^*) of these terminal residues. The H5/H6/H6′ connectivities are manifest in all spectra measured (Figures 2, 3, and 6).

Assignment of the rather evenly dispersed and favorably situated ceramide resonances was a matter of routine.

The above combined analysis showed the presence of nine different spin systems specified in Table I. Some of the coupling constants for β-Gal residues could not be determined because of cross-peak overlap and/or second-order effects.

The partial sequences and the sites of glycosidic linkages follow from the interresidue cross-peaks correlating the anomeric and the transglycosidic protons in the NOESY spectrum (Figure 7a). Although both H3 and H4 of Gal-VII residues showed interresidue NOE with H1 of Gal-VIII residues (Figure 7b), the linkages are obviously Galα1–3Gal [for references and discussion of this controversial problem, see Dabrowski et al. (1988)]. The same refers to the V1–3IV partial sequence. Additional interresidue cross-peaks that correlate IV1 and VIII1 with H6 and H6′ of the nearest aglyconic residues (Figure 7a) point to particular geometries of the relevant glycosidic bridges. A similar observation concerning the Galβ1–4Glc sequence in globoside was exploited in the determination of its three-dimensional structure (Scarsdale et al., 1986). Finally, *intra*residue H1–H3 and H1–H5 synaxial connectivities for β residues and H1–H2 axial–equatorial connectivities for α-Gal residues confirm the assignments for these protons (cf. Table I).

A careful integration of the 1D spectrum showed the presence of eight terminal α-Gal residues, which proves the octaantennary structure; the integrals of the Glc H1, Glc H2, and ceramide H5 resonances were used as unit values in the integration. In analogy with tri- (Dabrowski et al., 1984), tetra-, and pentaantennary neolactoglycosphingolipids (Hanfland et al., 1988), the gross branching pattern for **1** is assumed to conform with that represented by the general formula given in the abstract. In ~7% of the antennae α-Gal is lacking, as follows from the integral of the small H1 signal at 4.22 ppm (Figure 1), which corresponds to terminal β-galactose residues (Dabrowski et al., 1980).

It has been suggested that HOHAHA subspectra can be assigned by comparison of the splittings with those in the free monosaccharide or, in the case of unresolved resonances, by spectrum simulation using these splittings derived from free monosaccharides and the chemical shifts determined from the cross sections (Homans et al., 1987). Although this approach seems simple, it can hardly be of general applicability. First, the structure must somehow be known beforehand (or at least

anticipated), if coupling constants and chemical shifts for the proper monosaccharides are to be chosen for a comparison or simulation. Second, these chemical shifts can be misleading in view of the glycosylation-induced shifts occurring in oligosaccharides. Although, in principle, a trial-and-error procedure can be applied, this will be of little help, if alternative assignments produce a practically identical simulated spectrum, as in the case of H2, H3, and H4 in sugars of β-gluco configuration. These two points also apply to 1D HOHAHA spectra (Subramanian & Bax, 1987; Inagaki et al., 1987b; Lerner & Bax, 1987). Third, although fairly "pure" HOHAHA subspectra were obtained for some of the residues of a tetrasaccharide (Inagaki et al., 1987a) and even an oligomannoside (Homans et al., 1987), it is unrealistic to expect the same for all sugar residues of a complex oligosaccharide. In fact, cross-talk between cross sections may ruin a simulation by imitating false multiplets. At the same time, the cross-talk problem is alleviated in PS-COSY spectra, since the same coupling information can be obtained from different cross-peaks. As shown above, this coupling information is suitable for identifying the component sugars in an ab initio manner.

In conclusion, the combination of PS-COSY with the HOHAHA variant of total correlation spectroscopy is suggested as the most effective assignment strategy for oligosaccharides of great complexity.

ACKNOWLEDGMENTS

We thank Gisela Witzel for skillful technical assistance, Karin Trauner for preparing the figures, and Kristiane Derendorf for typing the manuscript.

Registry No. 1, 114633-52-2.

REFERENCES

Berman, E. (1987) *Eur. J. Biochem. 165*, 385–391.

Bodenhausen, G., Kogler, H., & Ernst, R. R. (1984) *J. Magn. Reson. 58*, 370–388.

Dabrowski, J. (1987) *Methods Stereochem. Anal. 9*, 349–386.

Dabrowski, J., Hanfland, P., & Egge, H. (1980) *Biochemistry 19*, 5652–5658.

Dabrowski, J., Hanfland, P., & Egge, H. (1982) *Methods Enzymol. 83*, 69–86.

Dabrowski, U., Hanfland, P., Egge, H., Kuhn, S., & Dabrowski, J. (1984) *J. Biol. Chem. 259*, 7648–7651.

Dabrowski, J., Ejchart, A., Kordowicz, M., & Hanfland, P. (1987) *Magn. Reson. Chem. 25*, 338–346.

Dabrowski, J., Hauck, M., Romanowska, E., & Gamian, A. (1988) *Carbohydr. Res.* (in press).

Davis, D. G., & Bax, A. (1985) *J. Am. Chem. Soc. 107*, 2820–2821.

Eich, G., Bodenhausen, G., & Ernst, R. R. (1982) *J. Am. Chem. Soc. 104*, 3731–3732.

Hanfland, P., Egge, H., Dabrowski, U., Kuhn, S., Roelcke, D., & Dabrowski, J. (1981) *Biochemistry 20*, 5310–5319.

Hanfland, P., Kordowicz, M., Peter-Katalinic, J., Egge, H., Dabrowski, J., & Dabrowski, U. (1988) *Carbohydr. Res.* (in press).

Hikichi, K. (1984) *JEOL News*, [*Ser.*] *Anal. Instrum. 20A*, 19–23.

Homans, S. W., Dwek, R. A., Fernandes, D. L., & Rademacher, T. W. (1984) *Biochim. Biophys. Acta 798*, 78–83.

Homans, S. W., Dwek, R. A., Boyd, J., Mahmoudian, M., Richards, W. G., & Rademacher, T. W. (1986) *Biochemistry 25*, 6342–6350.

Homans, S. W., Dwek, R. A., Boyd, J., & Rademacher, T. W. (1987) *Proc. Natl. Acad. Sci. U.S.A. 84*, 1202–1205.

Inagaki, F., Kohda, D., Kodama, C., & Suzuki, A. (1987a) *FEBS Lett. 212*, 91–97.

Inagaki, F., Kodama, C., Suzuki, M., & Suzuki, A. (1987b) *FEBS Lett. 219*, 45–50.

Koerner, T. A. W., Prestegard, J. H., & Yu, R. K. (1987) *Methods Enzymol. 138*, 38–59.

Kordowicz, M., Hanfland, P., Witzel, G., Dabrowski, U., Dabrowski, J., Peter-Katalinic, J., & Egge, H. (1986) *Abstracts of the XIIIth International Carbohydrate Symposium*, p 265, Cornell University, Ithaca, NY.

Lerner, L., & Bax, A. (1987) *Carbohydr. Res. 166*, 35–46.

Marion, D., & Wüthrich, K. (1983) *Biochem. Biophys. Res. Commun. 113*, 967–974.

Müller, L., & Ernst, R. R. (1980) *Mol. Phys. 38*, 963–992.

Perly, B., Bossenec, V., Berthault, P., & Petitou, M. (1987) *Tetrahedron Lett. 28*, 3331–3334.

Piantini, U., Sørensen, O. W., & Ernst, R. R. (1982) *J. Am. Chem. Soc. 104*, 6800–6801.

Prestegard, J. H., Koerner, T. A. W., Demou, P. C., & Yu, R. K. (1982) *J. Am. Chem. Soc. 104*, 4993–4995.

Rance, M., Sørensen, O. W., Bodenhausen, G., Wagner, G., Ernst, R. R., & Wüthrich, K. (1983) *Biochem. Biophys. Res. Commun. 117*, 479–485.

Romanowska, E., Gamian, A., Lugowski, C., Romanowska, A., Opferkuch, H. J., Dabrowski, J., & Hauck, M. (1987) *4th European Carbohydrate Symposium*, Darmstadt (Lichtenthaler, F. W., & Neff, K. H., Eds.) C-57, Gesellschaft Deutscher Chemiker, Frankfurt.

Scarsdale, J. N., Yu, R. K., & Prestegard, J. H. (1986) *J. Am. Chem. Soc. 108*, 6778–6784.

Subramanian, S., & Bax, A. (1987) *J. Magn. Reson. 71*, 325–330.

Wagner, G., & Wüthrich, K. (1979) *J. Magn. Reson. 33*, 675–680.